Journal of Materials Chemistry C

Accepted Manuscript

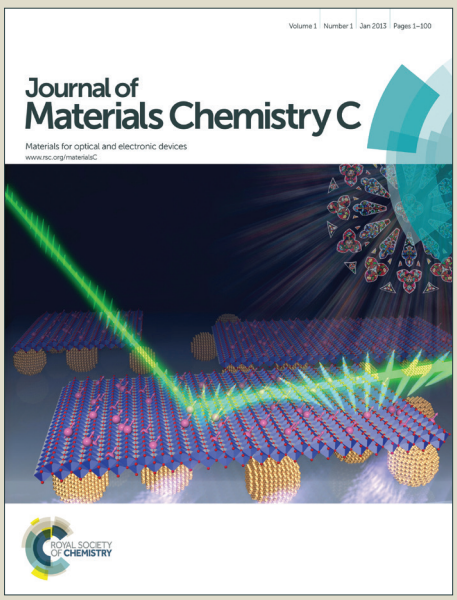

ROYAL SOCIETY OF CHEMISTRY

www.rsc.org/materialsC

Cite this: DOI: 10.1039/c0xx00000x

www.rsc.org/xxxxxx

ARTICLE TYPE

Bendable transparent ZnO thin film surface acoustic wave strain sensors on ultra-thin flexible glass substrates

Jinkai Chen, Xingli He, Wenbo Wang, Weipeng Xuan, Jian Zhou, Xiaozhi Wang[a]*, S.R.Dong[a], Sean Garner[b], Pat Cimo[b], and J.K. Luo[c,a]*

Received (in XXX, XXX) Xth XXXXXXXXX 20XX, Accepted Xth XXXXXXXXX 20XX
DOI: 10.1039/b000000x

Flexible and transparent (FT) ZnO thin film based surface acoustic wave (SAW) devices using indium tin oxide (ITO) electrodes were fabricated on ultrathin flexible glass substrates. The influence of annealing process and ITO thickness on the optical properties and acoustic wave power transmission properties of the devices were investigated. The performance of the devices improved significantly when the annealing temperature was raised up to 300 °C. The flexible glass based SAW devices exhibited similar power transmission performance, but have better optical transmittance than those on rigid glass. These FT strain sensors worked well under various applied strains up to ±3000 με with fast response time, and showed excellent linearity of resonant frequency with the change of strain with a sensitivity of ~34 Hz/με. The strain sensors demonstrated excellent stability and reliability under cyclic bending. The results demonstrated great potential of applications of the FT-SAW device based strain sensors on flexible glass substrates.

1 Introduction

Flexible and transparent (FT-) electronics are an emerging technology with great potential and innovation for applications owing to their excellent properties and advantages over traditional solid state electronics. Recently, many novel flexible electronic devices and microsystems have been developed such as flexible electronic displays, [1] electronic skin, [2] and eyeball cameras,[3] *etc*. Polymers such as polyethyleneterephthalate (PET), polyimide (PI), and polymethylmethacrylate (PMMA) are the most commonly used flexible substrates. They can endure large bending and strains, but have poor mechanical strength, wear resistance and thermal stability with typical working temperatures below 100 °C. Some of them have poor transparency as well, limiting their applications to the flexible regime only. Glass substrates are often used to develop transparent electronics, but they are rigid, not suitable for flexible electronics. Recently Corning has developed an ultrathin flexible glass, Corning® Willow® Glass, which has the combined merits of flexibility, transparency, high mechanical reliability and thermal stability, and high wear and corrosion resistance. Many applications based on Willow Glass have been explored.[4,5,6] In this work, we use this type of flexible glass as the substrate to fabricate flexible and transparent ZnO thin film surface acoustic wave (SAW) devices, and develop SAW-based high sensitivity strain sensors with extremely broad strain ranges.

SAW devices are a building block for electronics and microsystems, and have been extensively explored for applications such as radio frequency (RF) filters,[7] RF-ID tags,[8] microfluidic systems[9,10,11] and sensors for various physical[12,13] and biochemical sensing[14,15] *etc*. SAW devices are normally fabricated on bulk piezoelectric (PE) materials like $LiNbO_3$, $LiTaO_3$, or on piezoelectric thin films such as ZnO and AlN deposited on rigid substrates. Metals such as gold (Au) and aluminium (Al) are commonly used to fabricate the interdigitated transducers (IDTs). The use of rigid substrates and metal IDT electrodes make SAW devices not suitable for flexible and transparent electronic applications. We have recently developed SAW devices on flexible PI and rigid glass substrates using Al or Al-dope ZnO (AZO) as the electrodes,[13,16-18] and demonstrated their usability for communication, sensors and microfluidics. Here we report FT-SAW devices made on transparent and ultra-thin flexible glass using indium tin oxide (ITO) as the IDT electrodes. We will show the FT-SAW devices have better transparency and excellent flexibility than those on rigid glass and polymer substrates, and have great potential for FT-electronics and extremely wide range strain sensor applications.

2 ZnO and ITO films characterization and strain sensing setup

Willow Glass with a thickness of 100 μm and rigid glass (Corning 2318, 500 μm) were used as the substrates for the device fabrication. The diameter of both the flexible glass and rigid glass wafers was 100 mm. Nanocrystalline ZnO thin films with (0002) crystal orientation were deposited on the substrates by sputtering. Rigid glass was also used to fabricate the SAW devices for comparison. The deposition conditions for the ZnO films were fully optimized through our previous work,[16,17] and were used directly except the deposition temperature which was 100 °C for this work. It was found the crystal structure and optical properties

of the nanocrystalline ZnO films deposited on flexible glass are very similar to those on rigid glass and PI substrates, therefore they will not be discussed here in detail. For detailed information, please refer to our previously work.[16,17]

Conductive ITO thin film was used to fabricate the IDT electrodes using conventional ultraviolet light photolithography and lift-off process as it has better electrical conductivity than that of AZO.[17] The direct-current (DC) reactive magnetron sputtering was employed to deposit the ITO films using Argon plasma (the Ar flow rate was 100 sccm) and an ITO target (In_2O_3 90 wt.%:SnO_2 10 wt.%). The sputtering pressure, power, substrate temperature and bias voltage were optimized to be 0.70 Pa, 150 W, 100 °C and -75 V, respectively. The wafers were then annealed at 200 and 300 °C, respectively, for 10 minutes by rapid thermal annealing (RTP-CT100M) in N_2 at atmospheric pressure. For optical transmittance measurements, ITO was deposited on the surface of the ZnO layer on glass substrates. For the fabrication of IDT electrodes, the ZnO/Si wafers were patterned using photolithography, and ITO was deposited on the patterned wafers. After deposition of ITO, the wafers were immersed in acetone to remove unwanted ITO layer, and then they were annealed at various temperatures.

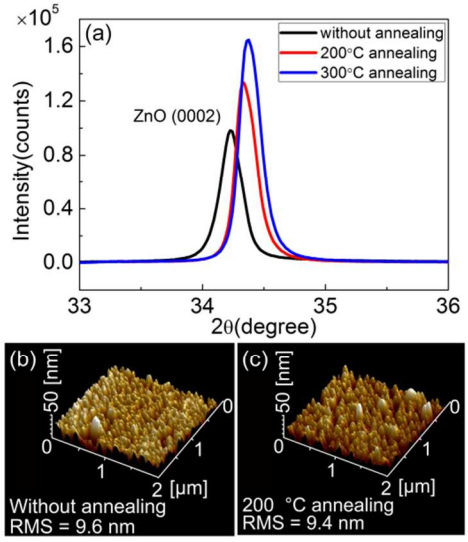

Fig. 1 (a) An XRD image comparing ZnO film before and after annealing (200 °C and 300 °C). AFM surface image of ZnO films before annealing (b) and after 200 °C annealing (c).

The crystalline orientation and surface morphology of the ZnO piezoelectric films before and after annealing was characterized using atomic force microscope (AFM, SPI-3800N, Seiko, Co.) and X-Ray diffraction (XRD, Panalytical Empyrean), respectively. Fig. 1(a) shows the XRD curve of the ZnO films before and after annealing. All the samples show (0002) ZnO crystalline orientation, and the intensity increase after annealing at 200 and 300 °C. Higher XRD intensity indicates better crystalline quality and fewer defects. The peak angle is 34.23°, 34.33° and 34.38° for the ZnO films without and with 200 °C, 300 °C annealing, respectively. The full-width at half maximum (FWHM) is 0.217°, 0.208° and 0.195° for the ZnO films without and with 200 and 300 °C annealing, respectively. The grain size of the ZnO films was calculated using the Debye-Scherrer formula[19],

$$D = 0.94\lambda_x/(\beta \cos\theta) \quad (1)$$

where D is the mean crystallite gain size normal to the diffracting plane. λ_x is the X-ray wavelength (1.54 Å for the Cu target), β is the HWFM in radians and θ represents the Bragg angle. The annealing process results in larger grain size which increases slightly from 39.99 nm (without annealing) to 41.74 and 44.53 nm (200 and 300 °C annealing). Larger grain size means fewer grain boundaries and interfacial defects. The surface roughness of the ZnO film is 9.6 nm (without annealing) and 9.4 nm (200 °C annealing) as shown in Fig. 1(b) and Fig. 1(c), respectively, and is comparable to those on Si and rigid glass substrates.

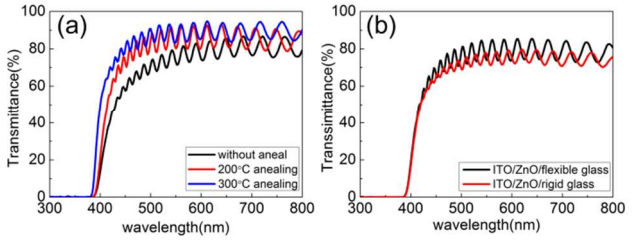

Fig. 2 Comparison of the optical transmittance for ITO(750 nm)/ZnO(2.5 μm) films with different annealing conditions (a), for the ITO/ZnO/flexible glass and ITO/ZnO/rigid glass structures (b).

It was found that annealing at 200 and 300 °C could also change the optical transmittance of the ITO(750nm)/ZnO(2.5μm) layers, significantly, from ~78% to ~89% in the visible light range as shown in Fig. 2(a). The improvement in optical transmittance is attributed to the growth of crystalline phases of the ITO[20] and ZnO[21] films, and the reduction of defects in the films during annealing. As shown in Fig. 2(b), the average optical transmittance of the stack of the ITO(750nm)/ZnO(2.5μm)/ flexible glass substrate after 200 °C annealing is over 80%, higher than the same structure on the rigid glass substrate (75%) in the visible light region,[17] owing to the ultrathin thickness of the flexible glass compared to the 500 μm thick rigid glass. Fig. 3(a) is a photograph of the ITO IDT electrode of the FT-SAW device, and Fig. 3(b) is an image of a bent flexible glass wafer with fabricated SAW devices, showing excellent optical transmittance and bendability.

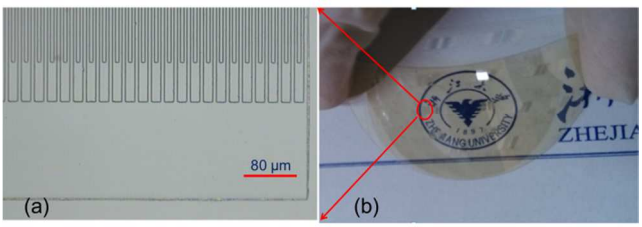

Fig. 3 A zoomed-in photograph of ITO IDTs (a) and photograph of the flexible glass wafer with fabricated SAW devices on flexible glass (2 inch in diameter) (b).

Fig. 4(a) is the setup for strain sensing experiments. As shown in Fig. 4(b), the SAW devices (3 mm × 4 mm) were bonded to a PCB board using conductive adhesive (MCN-DJ002) and electrically connected to SMA connectors. They together were glued on a flexible steel bar. A standard full-bridge strain gauge (BF1000-3h, 5 mm×5 mm) was assembled next to the PCB board to measure the strain. The strain gauge data were transferred to a computer through electrical connects. As shown in Fig. 4(a), a movable robotic arm (HSV-500) was used to bend the steel bar with SAW device and strain gauge assembly, and the SAW devices on the PCB board were electrically connected to a vector network analyzer (E5071C) to measure the RF power transmission properties of the SAW devices when strain is applied. A LabVIEW based program was developed to implement automated measurements of frequency shift of the devices.

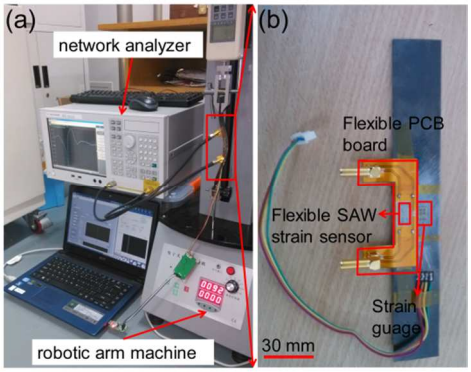

Fig. 4 A photograph of the setup for bending test (a), and a zoomed-in image of the strain sensor on the steel bar (b).

3 Power transmission property

The power transmission properties of the FT-SAW devices were characterized and compared with the SAW devices on the rigid glass substrate. Fig. 5 is the comparison of the power transmission spectrum of the SAW devices on both glass substrates. The wavelengths, λ, of the devices are 20 and 24 μm, respectively; the thickness of the ITO layer is 750 nm, and that of ZnO is 2.5 μm. The resonant frequency, f_r, of the Rayleigh wave was found to be 113.5 and 133.2 MHz for the SAW devices on the flexible glass with wavelengths of 24 μm and 20 μm, respectively, while that decrease to 109.5 and 129.4 MHz on the rigid substrate. As these devices on different substrates were fabricated at the same time using the same conditions, the higher resonant frequencies is believed to be due to the high acoustic velocity in the flexible glass or the thinner substrate (mass loading effect). All the devices have the amplitude of the resonant peaks over 20 dB, demonstrating their potential for applications in electronics, communications and sensors. The results show that the SAW devices on the flexible glass have higher f_r and a similar RF power transmission compared to those on rigid glass, therefore they are more suitable for FT-electronic application.

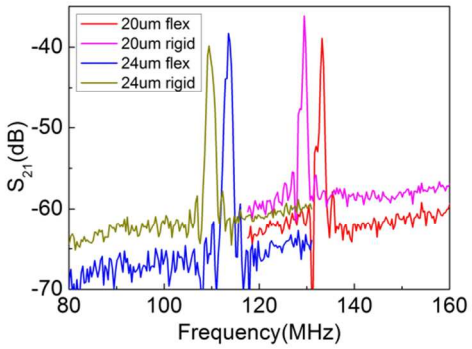

Fig. 5 Comparison of power transmission spectrum for the SAW devices with different wavelengths on both the flexible glass and rigid glass substrate.

The thickness of the ITO layer and the annealing temperature were varied to investigate their effects on the device performance. Table I summarizes the influence of the ITO thickness on the sheet resistance of the ITO films. The average sheet resistance decreases from 20.7 Ω/□ to 6.7 Ω/□ when the ITO thickness is increased from 250 nm to 750 nm. With the increase in ITO thickness, the power transmission property of the devices (not annealed) improves significantly as shown in Fig. 6(a). The insertion loss of the resonance decreases from ~-52 dB to ~-39 dB (the signal amplitude increases) when the ITO thickness is increased from 250 nm to 750 nm. Furthermore, the effective electromechanical coupling coefficient (k_{eff}^2) also increases dramatically (Table I) with the ITO thickness, with a tendency similar to that of the SAW devices with the AZO IDTs.[17] The decrease of the resonant frequency, as the ITO thickness is increased, is caused by the mass loading effect.[17]

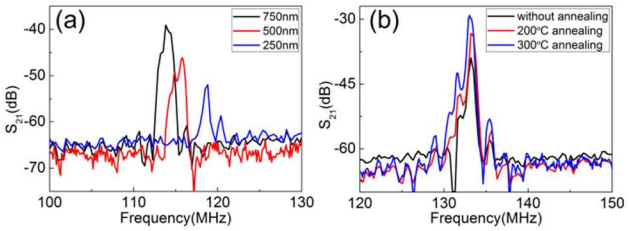

Fig. 6 Effect of the thickness of the ITO film on the power transmission spectrum of the devices without annealing (a), and influence of the annealing temperature on the power transmission spectrum (b).

Table I Summary of the ITO films and characteristics of the SAW devices with ZnO layer annealed at 200 °C.

λ(μm)	ITO thick. (nm)	$R_{□}$ (Ω/□) as-depo.	$R_{□}$ (Ω/□) (200 °C)	f_r (MHz) (200 °C)	k_{eff}^2(%) (200 °C)
24	250	20.7	10.5	118.8	0.97
	500	11.0	5.6	115.8	1.38
	750	6.7	4.7	113.8	1.58
20	250	20.7	10.5	139.1	0.78
	500	11.0	5.6	136.1	1.38
	750	6.7	4.7	133.2	1.54

After annealing at 200 °C, the sheet resistance decreases to 10.5, 5.6, and 4.7 Ω/□ for 250, 500, 750 nm ITO films, respectively, as summarized in Table I. This has great impact to the power transmission property of the SAW devices as shown in Fig. 6(b). The insertion loss of the resonance decreases (signal amplitude increases) from -38.92 of the unannealed sample to -33.28 and -29.10 dB after 200 and 300 °C annealing, respectively. The improvement of the power transmission characteristics by annealing is attributed to the improvement of crystal quality of ITO[20,22] and ZnO[23] films, increased grain sizes, reduced grain boundaries and defects, *etc*, that act as scattering centres to attenuate the acoustic waves.

4 Strain sensor

Since the ultra-thin glass is very flexible, the SAW devices on it are particularly suitable for the development of strain sensors with wide strain range, hence the performance of the devices (only those annealed at 200 °C) under various bending conditions were investigated. The resonant frequency of the devices responds rapidly with the change of strain, more work is undergoing to measure the rise and fall times. For simplicity, we introduce a unit of microstrain,[12,24,26,27] με, which is defined as με=(Δl/l)x10^6, where Δl and l is the change of length and the length of the device.

The cyclic test of the resonant frequency of the device (750 nm ITO, λ=20 μm) under tens of times repeated bending is shown in Fig. 7 with the strain varied from 0 to 2300 με (tensile strain). The red line represents the average resonant frequency under tensile strain, and the blue line is the average resonant frequency with no strain applied. The resonant frequencies with and without strain applied remain almost unchanged. We conducted the cyclic test for the devices several times, and found that as long as the strain is within 3000 με, the devices maintain the same performance without noticeable deterioration, demonstrated its high reliability and repeatability. However, when the strain reaches 3500 με or more, some devices show deterioration of the performance up on cyclic tests. Detailed investigation by optical microscope and SEM shows the ZnO film cracks. The number and the sizes of the cracks increase with strain. Although the SAW devices still resonate once the strain is withdrawn, the transmission amplitudes decrease accordingly depending on the strength of the strain applied. Therefore, we have restricted the strain to 3000 με for the following experiments.

The performance of the devices (750 nm ITO, λ=20 μm) under both the compressive and tensile strains was investigated. As shown in Fig. 8(a), the resonant frequency responds dynamically when the compressive strain changes in a step of 500 με. The frequency decreases about 110 kHz when the applied compressive strain is increased from zero to -3044.6 με. When the strain becomes tensile, the resonant frequency increases, as depicted by Fig. 8(b), opposite to the situation under compressive strain as expected.

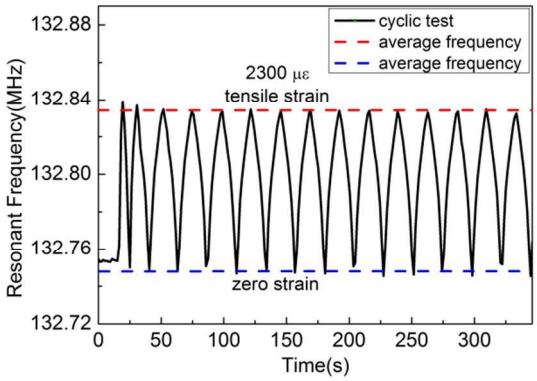

Fig. 7 The real time cyclic test of the SAW sensor under a repeated strain change from 0 με to 2300 με (tensile strain) with one cyclic duration of 25 s.

Fig. 8(c) shows the dependence of resonant frequency shift on strain from compression to tensile. The resonant frequency shift of the device exhibits a linear relationship for the whole strain range with a linear regression coefficient of 0.9949. The strain sensitivity, *Z*, of the device is defined as

$$Z = \Delta f / \Delta s \qquad (2)$$

where Δf and Δs are the absolute frequency shift and strain change of the device, respectively. The sensitivity of the devices can be calculated to be *Z*~34.7 Hz/με. Although the sensitivity is not as good as those of the SAW devices made on other piezoelectric substrates, the detectable strain range is at least 5 times larger than those that have the rigidity and fragility limitation, [12,24-27] clearly demonstrating their great potential for application in wide range strain sensing. Furthermore the sensitivity can be improved by using a thicker ZnO thin film layer for SAW devices as demonstrated by Nalamwar *et al*[31] and our work on other SAW sensors and actuators.[10,16]

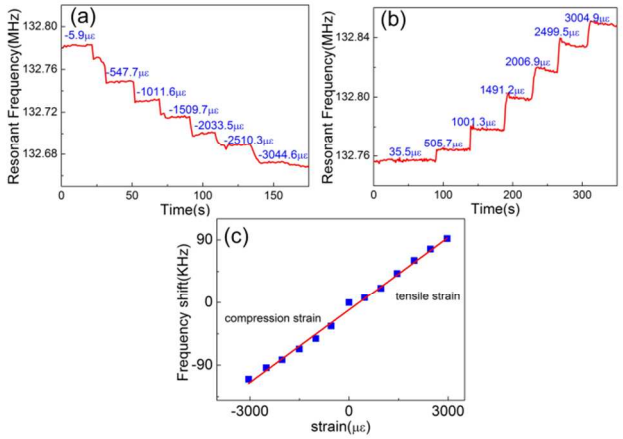

Fig. 8 Real-time responses of the device (750 nm ITO, λ=20 μm) under stepwise compression (a), tensile strain (b) and a summary of the frequency shift as a function of strain from compression to tensile, showing an excellent linearity (c).

The change of the resonant frequency of the devices with strain is determined by two factors: the change of wavelength caused by the deformation of the device surface and the IDT pitch, and the change of acoustic velocity induced by the change of the elastic modulus of the multilayer structure and material density under the applied stress.[28, 29, 30] Therefore the strain induced frequency shift will be the result of the combined effects. Assume the stress of the device surface is uniform which should be true for our case as the steel bar is much longer and stronger than the SAW device and PCB board, so that the SAW device can be bent uniformly, then the wavelength change under a strain of ε can be estimated by,

$$\lambda' = \lambda \times (1 \pm \varepsilon) \quad (3)$$

where λ and λ' are the wavelengths before and after bending, and the plus sign and minus sign correspond to the case of tensile and compressive strain, respectively. The acoustic velocity changes linearly with strain, and the ratio of the fractional velocity change $((v' - v)/v)$ to strain is approximately ~1.3/ε for the ZnO/glass layered structure.[31] The velocity in a strained substrate can be expressed as

$$v' = v \times (1 \pm 1.3 \times \varepsilon) \quad (4)$$

where v and v' are the acoustic velocities before and after bending, the plus sign and minus signs are for the tensile and compression strain, respectively. The frequency shift can be calculated as a function of strain applied with the result shown in Fig. 10. The surface deformation induced frequency shift decreases when the strain increases from compression to tensile, while that by acoustic velocity change is opposite for this ZnO/flexible glass double-layer structure as the fractional velocity change increases in ZnO/glass structure with the increase in strain.[30] The latter is offset by the effect of the surface deformation, reducing the strain sensitivity of the device. The theoretically calculated frequency shifts with the combined effects are in excellent agreement with the experimental results, clearly indicating the combined effects on the frequency shift of the SAW devices. We have tested five devices with the different wavelengths, all of them showed similar behaviour with good uniformity and repeatability.

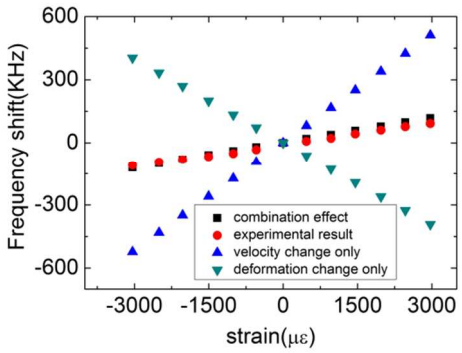

Fig. 9 Comparison of experimental result with the theoretically calculated frequency shift of a SAW device (λ=20 μm) in a strained ZnO/flexible glass structure. The ZnO thickness is 2.5 μm.

5 Conclusions

The flexible and transparent SAW devices based on ITO/ZnO/flexible glass structure have been fabricated, and devices with higher optical transmittance and better RF Power transmission property have been obtained after annealing at 200 and 300 °C. Most of the signal amplitudes of the Rayleigh resonances exceeded 20 dB, and the performance improves significantly when a thick ITO layer of 750 nm is used for the IDTs. The flexible glass substrate devices have similar power transmission properties to those made on rigid glass, but have much better optical transmittance and flexibility. The SAW devices showed excellent flexibility, stability and repeatability when subjected to a repeated bending. The flexible SAW sensors also demonstrated the tremendous capability to detect strains in a very wide range from -3000 to 3000 με (~ 5 times larger than others) with a sensitivity of ~34.7 Hz/με. All the results demonstrated its great potential for applications.

Acknowledgements

This work was supported by NSFC (No.61274037 and 61301046), Research Fund for the Doctoral Program of Higher Education of China (Nos. 20120101110031 and 20120101110054) and the Zhejiang Provincial NSF (No.Z11101168). The authors also would like to acknowledge the support by the Innovation Platform of Micro/Nanodevices and Integration System, Zhejiang University.

Notes and references

[a] *Dept. of Info. Sci. & Electron. Eng., Zhejiang University and Cyrus Tang Center for Sensor Mater. & Appl., 38 Zheda Road, Hangzhou 310027, P.R. China.E-mail: xw224@zju.edu.cn*
[b] *Corning Incorporated, One River Front Plaza, Corning, NY 14831, USA.*
[c] *Inst. of Renew. Energ. & Environ. Technol., University of Bolton, Deane Road, Bolton, BL3 5AB, U.K.E-mail: jl2@bolton.ac.uk*

[1] S. I. Park, Y. J. Xiong, R. H. Kim, P. Elvikis, M. Meitl, D. H. Kim, J. Wu, J. Yoon, C. J. Yu, Z. J. Liu, Y. G. Huang, K. Hwang, P. Ferreira, X. L. Li, K. Choquette, and J. A. Rogers, *Sci.,* 2009, **325,** 977.
[2] T. Someya, T. Sekitani, S. Iba, Y. Kato, H. Kawaguchi, and T. Sakurai, *Proc. Natl. Acad. Sci. U.S.A.* 2004, **101,** 9966.
[3] H. C. Ko, M. P. Stoykovich, J. Z. Song, V. Malyarchuk, W. M. Choi, C. J. Yu, J. B. Geddes, J. L. Xiao, S. D. Wang, Y. G. Huang, and J. A. Rogers, *Nat.,* 2008, **454,** 748.
[4] S. Hoehla, S. Garner, M. Hohmann, O. Kuhls, X. H. Li, A. Schindler, and N. Fruehauf, *J. Disp. Technol.,* 2012, **8,** 309.
[5] S. Garner, M. Q. He, P. Y. Lo, C. F. Sung, C. W. Liu, Y. M. Hsieh, R. Hsu, J. M. Ding, J. P. Hu, Y. J. Chan, J. J. ChiehLin, X. H. Li, M. Sorensen, J. F. Li, P. Cimo, and C. K. TingKuo, *J. Disp. Technol.,* 2012, **8,** 590.
[6] W. L. Rance, J. M. Burst, D. M. Meysing, C. A. Wolden, M. O. Reese, T. A. Gessert, W. K. Metzger, S. Garner, P. Cimo, and T. M. Barnes, *Appl. Phys. Lett.,* 2014, **104,** 143903.
[7] U. C. Kaletta, P. V. Santos, D. Wolansky, A. Scheit, M. Fraschke, C. Wipf, P. Zaumseil, and C. Wenger, *Semicond. Sci. Technol.,* 2013, **28**.
[8] V. P. Plessky and L. M. Reindl, *IEEE Trans. Ultrason. Ferroelectr.,* 2010, **57,** 654.

[9] Y. Q. Fu, J. K. Luo, X. Y. Du, A. J. Flewitt, Y. Li, G. H. Markx, A. J. Walton, and W. I. Milne, *Sensor. Actuat. B,* 2010, **143,** 606.
[10] X. Y. Du, Y. Q. Fu, J. K. Luo, A. J. Flewitt, and W. I. Milne, *J. Appl. Phys.,* 2009, **105,** 024508.
[11] H. F. Pang, Y. Q. Fu, L. Garcia-Gancedo, S. Porro, J. K. Luo, F. Placido, J. I. B. Wilson, A. J. Flewitt, W. I. Milne, and X. T. Zu, *Microfluid. Nanofluid.,* 2013, **15,** 377.
[12] B. Donohoe, D. Geraghty, and G. E. O'Donnell, *IEEE Sens. J.,* 2011, **11,** 1026.
[13] X. L. He, D. J. Li, J. Zhou, W. B. Wang, W. P. Xuan, S. R. Dong, H. Jin, and J. K. Luo, *J. Mater. Chem. C,* 2013, **1,** 6210.
[14] D. S. Lee, J. H. Lee, J. K. Luo, Y. Q. Fu, W. I. Milne, S. Maeng, M. Y. Jung, S. H. Park, and H. C. Yoon, *J. Nanosci. Nanotechnol.,* 2009, **9,** 7181.
[15] T. M. A. Gronewold, *Anal. Chim. Acta.,* 2007, **603,** 119.
[16] H. Jin, J. Zhou, X. L. He, W. B. Wang, H. W. Guo, S. R. Dong, D. M. Wang, Y. Xu, J. F. Geng, J. K. Luo, and W. I. Milne, *Sci. Rep.,* 2013, **3,** 2140.
[17] J. Zhou, X. L. He, W. B. Wang, Q. Zhu, W. P. Xuan, H. Jin, S. R. Dong, D. M. Wang, and J. K. Luo, *IEEE Electron Dev. Lett.,* 2013, **34,** 1319.
[18] X. L. He, J. Zhou, W. B. Wang, W. P. Xuan, X. Yang, H. Jin, and J. K. Luo, *J. Micromech. Microeng.,* 2014, **24,** 055014.
[19] J. Zhou, X. L. He, H. Jin, W. B. Wang, B. Feng, S. R. Dong, D. M.Wang, G. Y. Zou, and J. K. Luo, *J. Appl. Phys.* 2013, **114**, 044502.
[20] R. Latz, K. Michael, and M. Scherer, *Jpn. J. Appl. Phys. Pt. 2.,* 1991, **30,** L149.
[21] P. Prepelita, V. Craciun, M. Filipescu, and F. Garoi, *Thin Solid Films,* 2013, **545,** 564.
[22] Y. L. Hu, X. G. Diao, C. Wang, W. C. Hao, and T. M. Wang, *Vac.,* 2004, **75,** 183.
[23] M. K. Puchert, P. Y. Timbrell, and R. N. Lamb, *J. Vac. Sci. Technol.* A, 1996, **14,** 2220.
[24] M. D. G. Potter, P. B. Kirby, M. Y. Lim, V. A. Kalinin, and A. Lonsdale, *Proc. 2002 IEEE Int. Freq. Contr. Symp. & Pda Exhib.*, 2002, 220.
[25] Z. Q. Bao, M. Hara, M. Mitsui, K. Sano, S. Nagasawa, and H. Kuwano, *Jpn. J. Appl. Phys.,* 2012, **51**,07GC23.
[26] R. Stoney, D. Geraghty, and G. E. O'Donnell, *IEEE Sens. J.,* 2014, **14,** 722.
[27] V. Kalinin, *Rawcon: 2004 IEEE Radio And Wireless Conf., Proc.,* 2004, pp.187.
[28] M. Epstein and A. L. Nalamwar, *IEEE Trans. Sonics. Ultrasonics.,* 1976, **23,** 219.
[29] A. L. Nalamwar and M. Epstein, *J. Appl. Phys.,* 1976, **47,** 43.
[30] A. L. Nalamwar and M. Epstein, *IEEE Trans. Sonics. Ultrasonics.,* 1976, **23,** 144.
[31] A. L. Nalamwar and M. Epstein, *IEEE Ultrason. Symp.*, 1974, 129-31.

We demonstrated the flexible SAW sensors based on ultra-thin glass have the tremendous capability to detect strains in a very wide range (~ 5 times larger than others) with a sensitivity of ~34.7 Hz/με.